energies

MDPI

Article

Core Temperature Estimation for a Lithium ion 18650 Cell

Sumukh Surya [1,*], Vinicius Marcis [2] and Sheldon Williamson [3]

1 e-PowerTrain, KPIT, Bangalore 560103, India
2 Advanced Storage Systems and Electric Transportation (ASSET) Laboratory, 11110 Artesia Blvd, Cerritos, CA 90703, USA; vinicius.marcis@ontariotechu.net
3 Department of Electrical, Computer, and Software Engineering, University of Ontario Institute of Technology, Oshawa, ON L1H 7K4, Canada; sheldon.williamson@uoit.ca
* Correspondence: sumukhsurya@gmail.com

Abstract: This paper deals with the estimation of core temperature (T_c) of a Lithium (Li) ion battery using measured ambient and surface temperatures. The temperatures were measured using thermocouples placed at appropriate locations. A second order thermal model was considered for the core temperature (T_c) estimation. A set of coupled linear ordinary differential equations (ODEs) were obtained by applying Kirchhoff's current and voltage laws to the thermal model. The coupled ODEs were redefined in the discrete state space representation. The thermal model did not account for small changes in surface temperature (T_s). MATLAB/Simulink were used for modelling a Kalman filter with appropriate process and measurement noise levels. It was found that the temperatures closely followed the current patterns. For high currents, T_c dominated the surface temperature by about 3 K. T_c estimation plays a very important role in designing an effective thermal management and maintaining the state of health (SOH) during fast discharges under limits. Most of the battery management system (BMS) applications required T_s as the input to the controller. Hence, an inverse calculation for estimating T_s from known T_c was carried out and found to be reasonably accurate. It was found that the thermal parameter C_s played a major role in the accuracy of T_s prediction and must have low values to minimize errors.

Keywords: battery core temperature; Kalman filter; Li ion battery; MATLAB/Simulink; thermal management system

Citation: Surya, S.; Marcis, V.; Williamson, S. Core Temperature Estimation for a Lithium ion 18650 Cell. *Energies* **2021**, *14*, 87. https://dx.doi.org/10.3390/en14010087

Received: 8 November 2020
Accepted: 23 December 2020
Published: 25 December 2020

1. Introduction

With fossil fuels depleting at a rapid rate, there is a need for automobiles to be driven from alternate sources of energy. A traditional automobile pollutes the environment by letting out harmful gases. A battery electric vehicle (BEV) does not require fossil fuels, is nonpolluting and has fewer moving parts requiring less maintenance than a conventional fossil-fuel powered vehicle. Hence, a BEV is considered superior compared to fossil-fuel powered cars. Hence, to maintain stable operation and obtain maximum power from a battery, temperature monitoring is called for. From practical considerations, it is not always possible to measure or monitor core temperature (T_c) and take corrective action. But surface temperature (T_s) and ambient temperature (T_{amb}) can be measured. In the present work, T_c of a battery was estimated using a Kalman filter. A thermal model of a battery was developed using convection resistances and convection capacitances. The governing equations for T_s and T_c were derived in terms of T_{amb} from the developed thermal model. Since, T_c cannot be measured directly, and estimation technique was used to predict it using a Kalman filter based on measured T_s and T_{amb} for different patterns of current. An inverse process of estimating T_s from known T_c was carried out and the role of the thermal parameter C_s was studied. Since, the changes in T_s were ignored, $dT_s/dt = 0$. Hence, C_s was not present in the state space equations. By integrating dT_s/dt, T_s was found in the inverse calculation.

Major Contributions: In this paper, T_c for a Li (Lithium) ion battery was estimated using a thermal model using a Kalman Filter. The changes in T_s for short intervals were ignored as they were very small. The thermal parameter C_s did not contribute to T_c. For all BMS applications, the sensed temperature, T_s is used as an input for the controller as homogeneity in T_s exits. Hence, an attempt was made to estimate T_s from known T_c so as to build a wireless BMS (battery management system). It was observed that the parameter C_s contributed to T_s as dT_s/dt was integrated to obtain T_s from estimated T_c. Lower C_s values provided better estimates for T_s.

2. Literature Review

Electric vehicle/hybrid electric vehicles (EV/HEV) generally use battery packs to drive vehicles. These battery packs are made of hundreds of cells connected in series and parallel combinations based on voltage and current requirement. Generally, Li ion cells are preferred due to several advantages like high energy density and high specific density [1]. However, they are highly sensitive to temperature (generally high temperature reduces battery life and capacity). Therefore, they must be operated under certain ranges of temperature for better performance and life [1].

In the past, several attempts have been made in estimating the T_c of the battery. A lithium iron phosphate ($LiFePO_4$) battery of 40 Ah capacity was selected and its T_c was estimated using a thermal model [2]. Three temperature sensors were placed at appropriate locations to estimate T_c. Surface temperature (T_s) sensors were placed at strategic locations and measured. The experiment was performed in a controlled temperature chamber and hence T_{amb} was fixed to 25 °C. The battery thermal parameters where found using the least square algorithm. It was found that the values of thermal parameters C_c and C_s did not contribute to the steady state temperature. However, their effect was predominant in the transient period of T_c estimation. Based on the thermal model, the governing equations were derived. A transfer function of T_c/Q was extracted. The ABCD matrices (state space matrices) were obtained and fed to the Kalman filter. The states were T_{is} and T_{ss} where T_{is} was T_c and T_{ss} was T_s.

MATLAB/Simulink was used for modelling and thermal parameters were obtained from experiments in [3,4]. A thermal model was developed based on the heat developed by (a) internal resistance Q_Ω, (b) rate of mixing of materials Q_{rev} and (c) environmental heat transfer Q_{env}. The equivalent battery parameters had two RC pairs and an internal resistance R_0 in series with open circuit voltage (OCV). It was observed that when the SOC ranged between 0.3 and 0.7, Q_{rev} became negligible. This phenomenon was observed during battery discharge. The limitation in this paper was that the effect of T_{amb} and the T_s was not considered. $LiFePO_4$ battery of 40 Ah capacity was selected.

The quantity of heat generated was taken as a product of current squared and an estimated value of resistance in [5]. The ABCD matrices were obtained from the derived thermal model. The states were T_c and T_s and the inputs were I^2 and T_{amb}. A Luenberger observer was used to estimate T_c based on output T_s. The thermal parameters were estimated using recursive least square (RLS) algorithm.

In order to estimate T_c, OCV, V_T, T_s and T_{amb} are required [6]. The OCV of a Li ion battery can be estimated using V_T. In this paper, the OCV was estimated using Thevenin's model as shown in [7]. However, fast charging applications, higher order battery models need to be used to estimate OCV [8]. A five RC pair enhanced self -correcting (ESC) model was used to capture the high frequency components in current.

T_c estimations were carried out mainly using a Kalman Filter (KF), finite element method (FEM) and extended Kalman filter (KF).

The general form of a KF and its governing equations are discussed in [9–11]. The output of the KF was T_c and the inputs were OCV, V_T, T_s and T_{amb} [8]. The governing equations for a KF is shown in [12].

The finite element method (FEM) was the numerical approach used to model the thermal behavior of batteries. FEM finds an approximate answer to boundary value problems for partial differential equations. The method takes the total problem area and divides it into a finite amount of elements and uses variation methods to solve the problem by minimizing the error [13–16]. The proposed model was based on Pade's approximation method and simplified thermal model. Pade's method computes total heat generation and this feeds the simplified thermal model. The rational transfer function of the reaction flux, surface concentration, electrolyte concentration and over potential at the boundary conditions (entire width of the battery) was computed to find V_T and OCV. Simultaneously, the thermal model estimated T_c.

A sensor-less method for estimation of T_c was proposed in [17]. An extended Kalman filter (EKF) was used to estimate T_s and T_c. The validation was carried out by comparing measured T_s with the estimated value. The thermal model considered was a PDE (partial differential equation) which was dependent on the geometry of the battery and thermal specifications. A 2.3 Ah LiFePO4 battery was considered.

3. Thermal Model

Figure 1 shows the thermal model considered for T_c estimation. It consists of thermal resistances R_c and R_u (K/W) and heat capacity at the core and surface regions C_c and C_s (J/K).

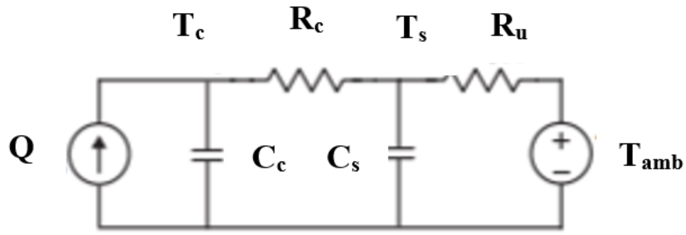

Figure 1. Second order thermal model of a battery [18].

Equations (1) and (2) are used to estimate the value of T_c for various current patterns

$$Cc\frac{dTc}{dt} = Q + (Ts - Tc)/Rc \tag{1}$$

$$Cs\frac{dTs}{dt} = (T_{amb} - Ts)/Ru - (Ts - Tc)/Rc \tag{2}$$

$$Ts = \int \left[\frac{T_{amb} - Ts}{Cs * Ru} - \frac{Ts - Tc}{Rc * Cs}\cdot\right] \tag{3}$$

$$Tc = \int \left[\frac{1}{Cc}\cdot Q + \frac{Ts - Tc}{Cc * Rc}\cdot\right] \tag{4}$$

$$Q = I * (V_T - V_{OCV}) \tag{5}$$

The state model of a KF are shown in (8) and (9)

$$X_k = A_{k-1} * X_{k-1} + B_{k-1}u_{k-1} + W_{k-1} \tag{6}$$

$$Y_k = C_k * X_k + D_k * U_k + V_k \tag{7}$$

where X_t is state of the system ($T_{c,t}$), Y_t = output of the system ($T_{s,t}$), u_t is the input to the system ($[T_{amb,t}\ Q]^T$), t = present state of the system and t − 1 = previous state of the system.

Rewriting Equations (1) and (2) in discrete time:

$$[\mathrm{T_{c,t}}] = \left[1 - \frac{1}{\mathrm{Cc\,(Rc + Ru)}}\right][\mathrm{T_{c,t-1}}] + \left[\frac{1}{\mathrm{Cc\,(Rc + Ru)}}\ \ \frac{1}{\mathrm{Cc}}\right]\begin{bmatrix} Q \\ Tf \end{bmatrix} \tag{8}$$

$$[\mathrm{T_{s,t}}] = \left[\frac{\mathrm{Ru}}{\mathrm{Rc + Ru}}\right][\mathrm{T_{c,t-1}}] + \left[\frac{\mathrm{Rc}}{\mathrm{Rc + Ru}}\ \ 0\right]\begin{bmatrix} Q \\ Tf \end{bmatrix} \tag{9}$$

LMX35 series from Texas Instruments was used to measure T_s and T_{amb} and the accuracy in the measurement was 1 K.

The governing equations of the Kalman filter were simulated using MATLAB/Simulink with the help of 'Commonly Used Blocks'.

4. Experimental Setup

A MATLAB script based automated battery test system (BAS) which runs on Windows 10 was used for the experimentation. This had the capability of providing 100 ms latency between real time experiment and the operational system. Since, the control is based on temperature response, which has latency in the range of minutes; it is possible to implement the controller in such manner. Figure 2 shows the components of BAS and their integration. The power paths are represented by solid lines, communication and signal paths are represented by dashed lines. Standard commands for programmable instruments (SCPI) protocol are used for controlling action. Table 1 shows the battery specifications.

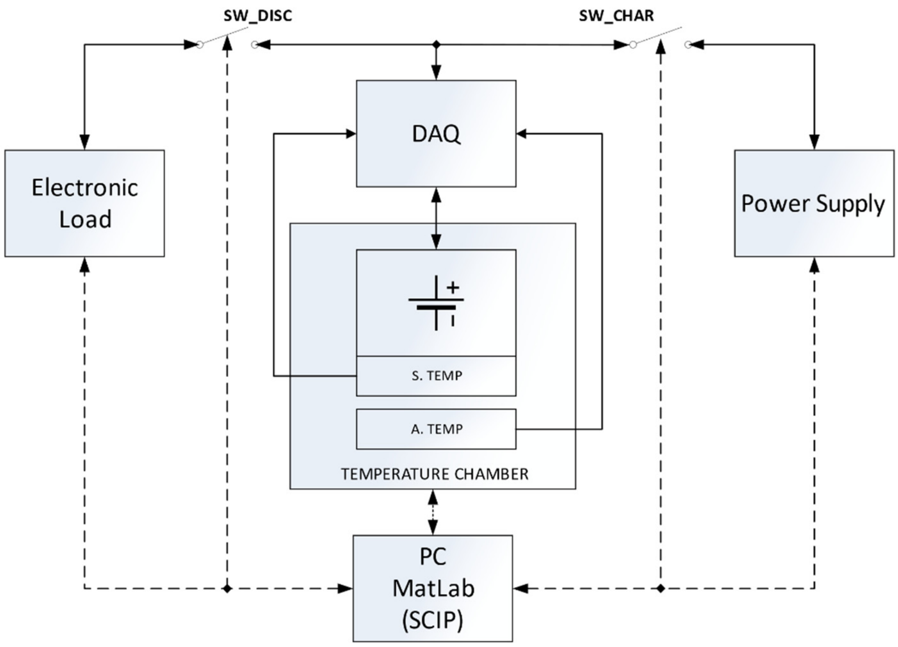

Figure 2. Block Diagram of a battery test system (BAS).

Table 1. Specifications of NMC (Lithium Nickel Manganese Cobalt Oxide) Lithium-ion battery.

Specifications	Values
Manufacturer	LG Chem
Model	INR18650HG2
Chemical System	LiNiMnCo02HNMC
Nominal Voltage	3.6 V
Nominal Capacity	3000 mAh
Standard Charging (CC-CV)	1.5 A, 4.2 V max, Cut Off: 50 mA
Fast Charging (CC-CV)	4 A 4.2 V max, Cut Off: 100 mA
Discharging Condition	20 A
Discharge Cut Off Voltage	2 V
Operating Temperature	Charge: 0 to 50 °C, Discharge: −30 to 60 °C
Weight	48 g

For charging the battery, a programmable power supply E36313A from Keysight was used. 6 A and 10 A were delivered at the first channel, with a least count of 350 μV. This provided four wire configurations helpful to remove the losses. Second and third channels were utilized to control the relays, SW_CHAR and SW_DISC as shown in Figure 2. In order to provide protection during charge and discharge cycles, relays were used. A detailed explanation regarding the setup is provided in [19]. Figure 3 shows the experimental setup for measurement of T_{amb}, T_s, Current and V_T.

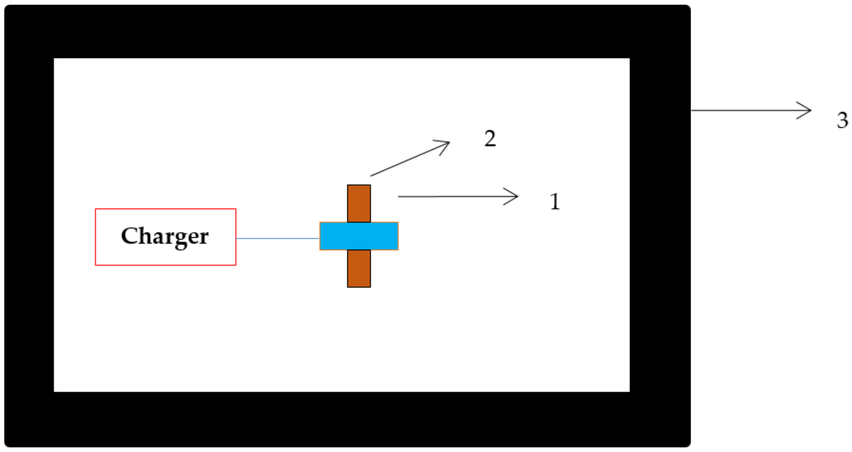

Figure 3. Schematic of experimental setup. 1. Battery under test. 2. Temperature Sensor. 3. Thermal chamber.

T_{amb} could be maintained at −273 K, 293 K and 323 K with an auxiliary temperature chamber from associated environmental system. It had the capability to operate in the range of 233 K to 358 K. The geometry of the battery had a diameter of 18.5 mm and height of 65.2 mm.

5. Results and Analysis

T_c was estimated using a KF for various patterns for currents depending on the datasheet for the Li ion cell so that no capacity fade occurred. Four test cases numbered 1 to 4, were considered. The results obtained are discussed below:

5.1. *Case 1*

The pattern of current is shown in Figure 4. T_c was initialized to T_s and T_{amb} = 273.4 K taken as the initial condition is shown in Figure 5. It may be noted that T_c and T_s closely followed the current pattern. As observed from Figure 6, T_c and T_s closely followed each other and the current profile. Figure 7 shows ($T_c - T_s$) with respect to time. As the rate of current drawn from the battery increased, T_c >> T_s and the maximum deviation was of the order of 5 K.

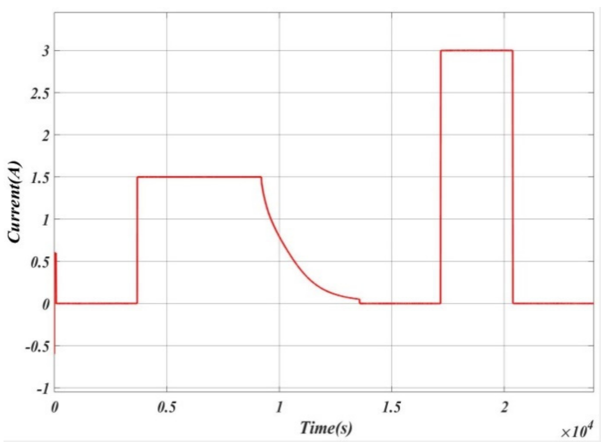

Figure 4. Current vs. Time.

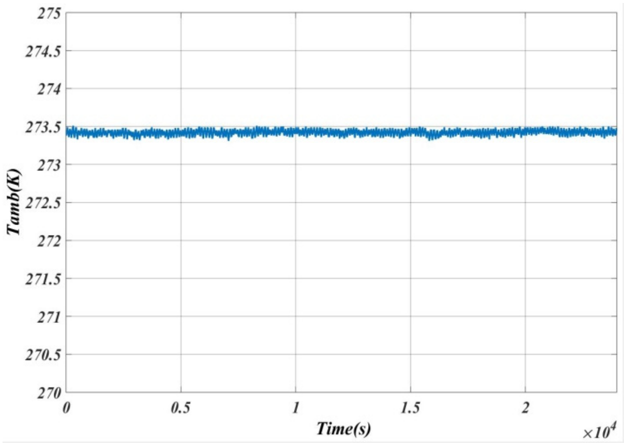

Figure 5. T_{amb} vs. Time.

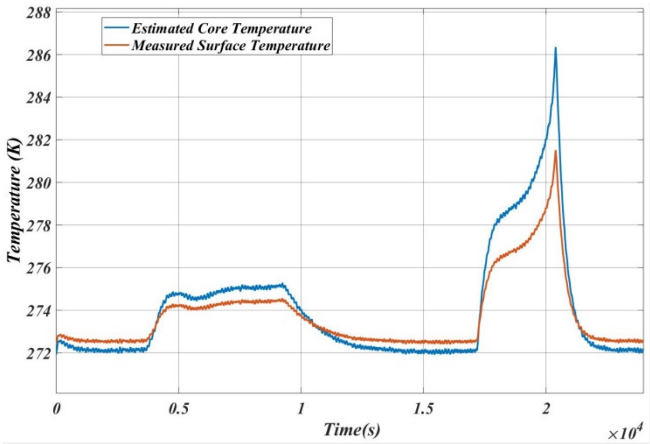

Figure 6. Variation of estimated T_c and measured T_s.

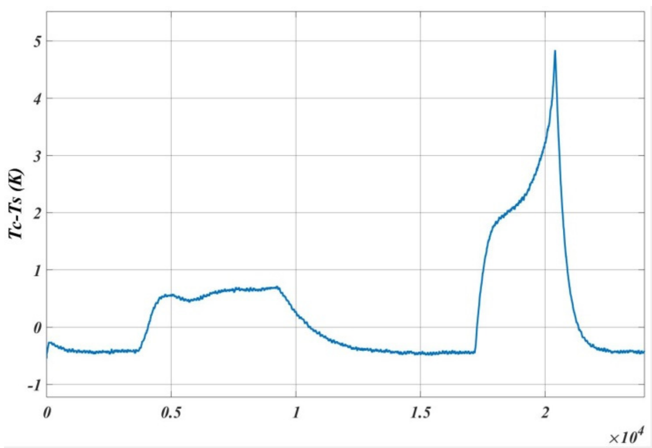

Figure 7. Variation of ($T_c - T_s$).

5.2. *Case 2*

In this case, the current profile was altered as shown in Figure 8. T_c was initialized to T_s and T_{amb} = 323 K as per Figure 9. Figure 10 shows the variation of T_c with respect to T_s and Figure 11 shows the difference between T_c and T_s as a function of time. It may be noted that T_c and T_s followed the current pattern, as in Case 1 and the maximum difference between T_c and T_s was about 1.5 K, which occurred when the current was maximum.

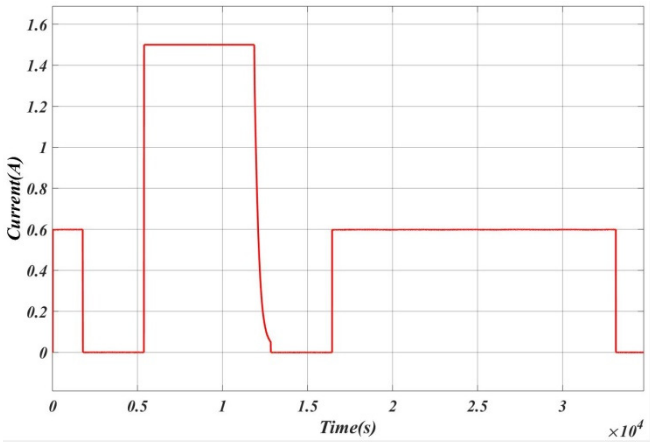

Figure 8. Current vs. Time.

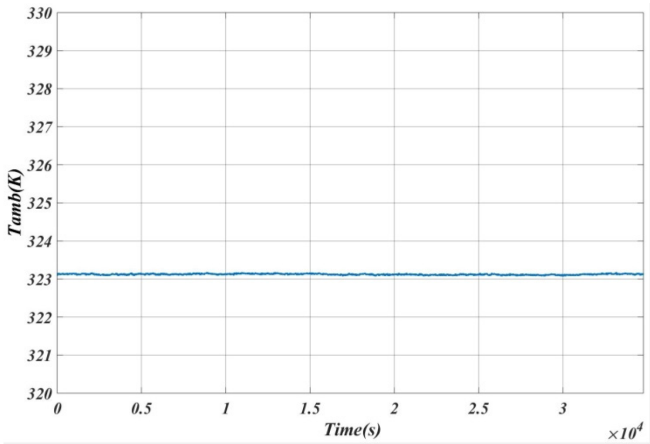

Figure 9. T_{amb} vs. Time.

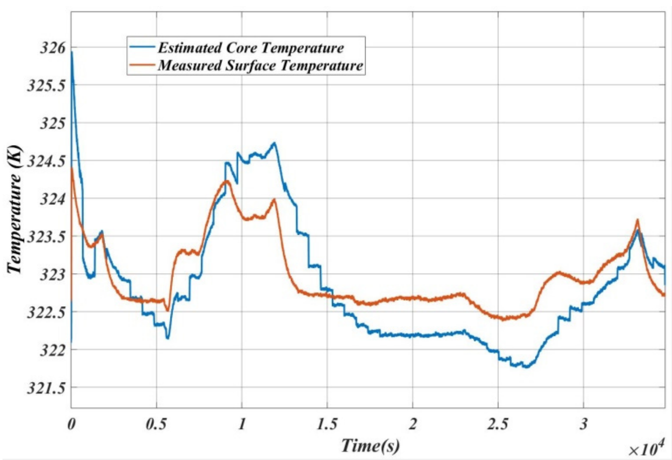

Figure 10. T_c and T_s vs. Time.

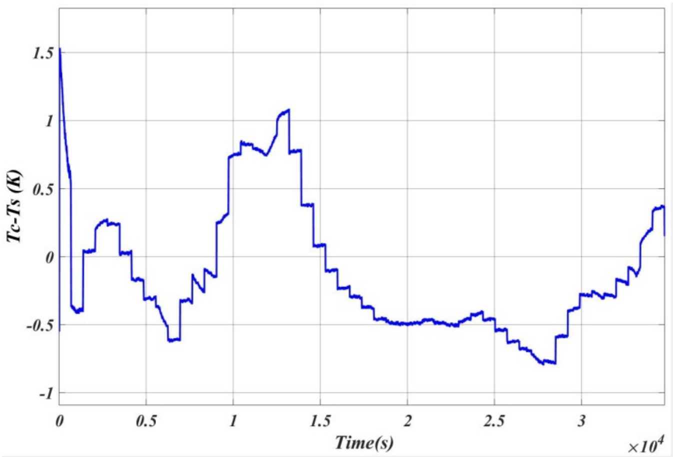

Figure 11. ($T_c - T_s$) vs. Time.

It may be noted from Case 1 and 2 studies, that the deviations in the estimates were relatively high (~5 K) whenever the current changed as a large step-function. It seems that the equations used cannot satisfactorily resolve such profiles.

5.3. *Case 3*

The profile of current discharge is shown in Figure 12. T_{amb} = 274 K was chosen, as per Figure 13. Figure 14 shows the estimated T_c and measured T_s variations. As the current rose to 0.6 A, T_c also increased to about 276 K causing a difference of about 1.2 K with respect to T_s. At lower current values, T_s dominated T_c and the difference was about 0.5 K. Figure 15 shows the difference between T_c and T_s.

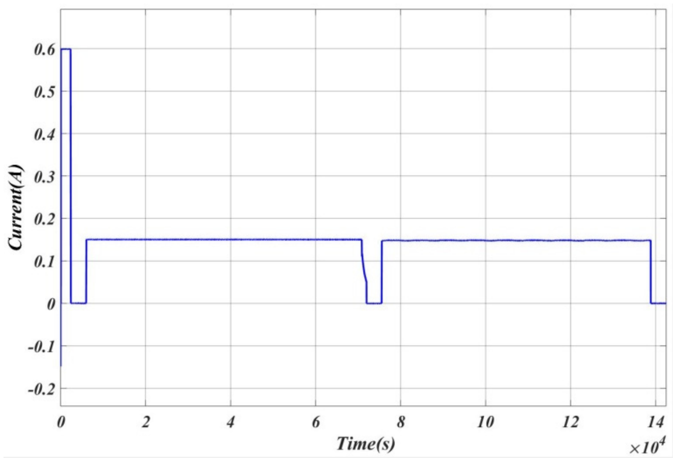

Figure 12. Current vs. Time.

5.4. *Case 4*

The current profile is shown in Figure 16. Figure 17 shows the T_{amb} variation. Figure 18 shows the variation of estimated T_c and measured T_s and Figure 19 shows the variations of ($T_c - T_s$). Since the rate of current discharge was very small, $T_s > T_c$ and difference was very small. Hence, it can be noted that at lower current discharges, $T_s > T_c$ which is shown in Figure 19.

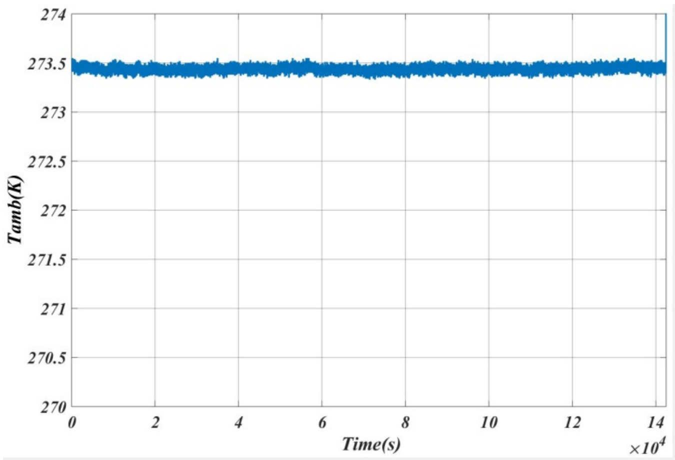

Figure 13. Variation of T_{amb}.

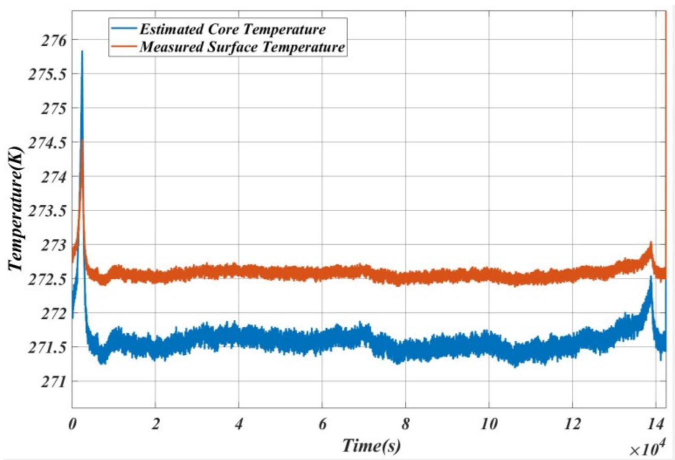

Figure 14. Variations of estimated T_c and measured T_s.

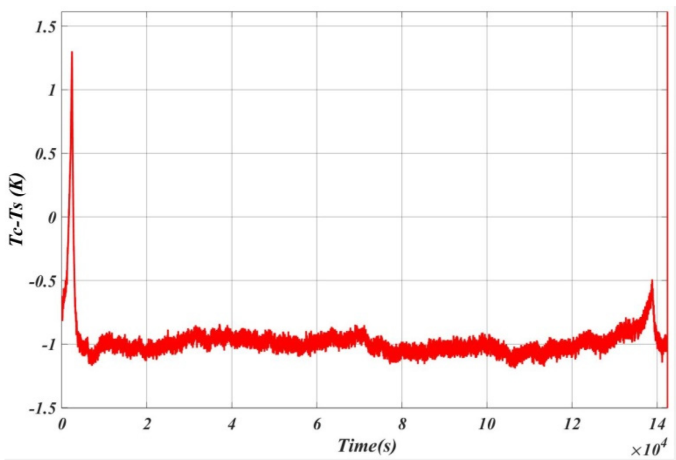

Figure 15. $(T_c - T_s)$ vs. Time.

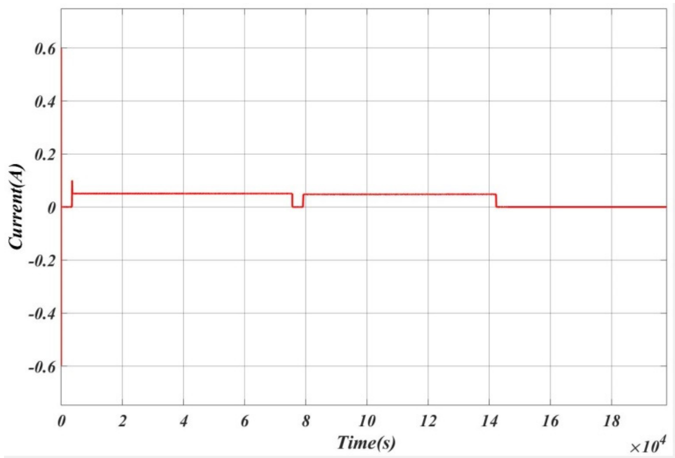

Figure 16. Current vs. Time.

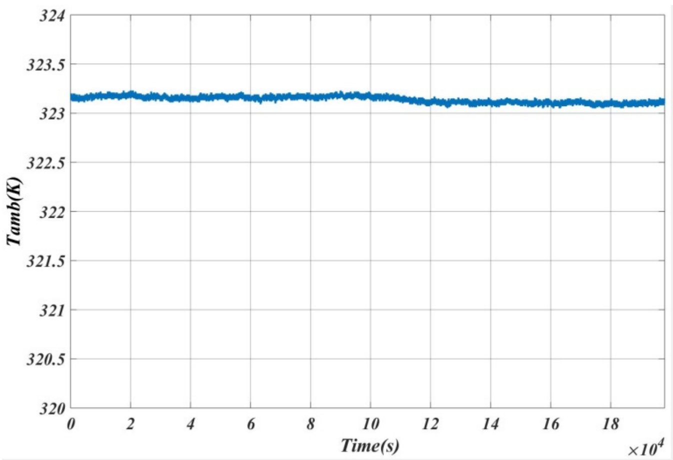

Figure 17. T_{amb} vs. Time.

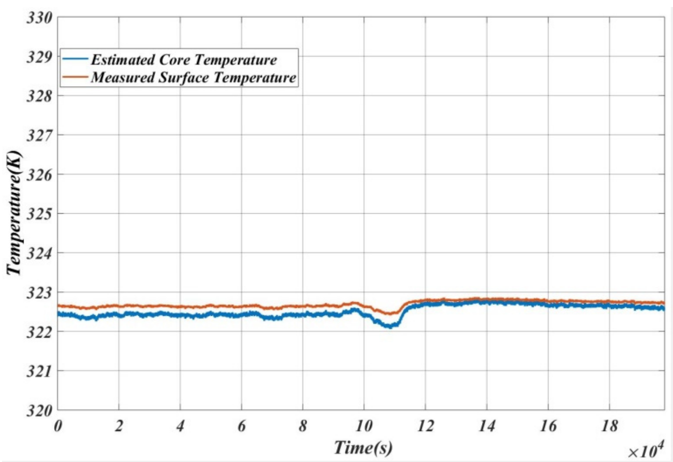

Figure 18. Estimated T_c and T_s vs. Time.

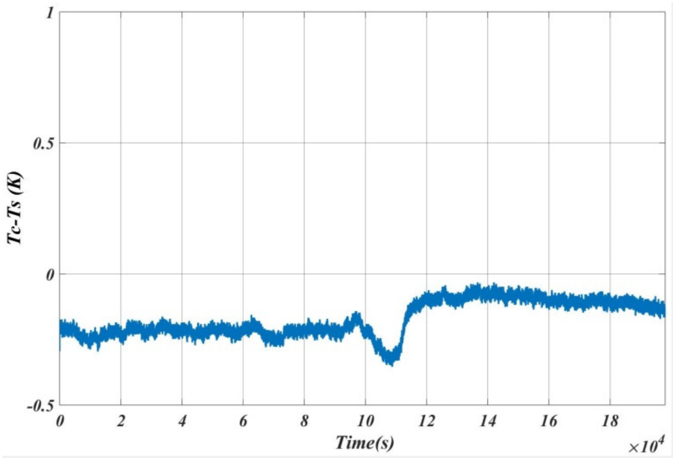

Figure 19. $T_c - T_s$ vs. Time.

As seen in Figures 14–19, a noisy response was observed. This noise in the signal was due to the temperature chamber cooling system and this had no effect on the temperature measurement.

6. Inverse Calculation for the Verification of the Algorithm

For verifying the algorithm, estimated T_c was used to predict and compare with measured T_s. The initial condition for recalculating T_s was based on that of T_c using Equation (5). The differences between $T_{c\ estimated}$ and $T_{c\ measured}$ were compared and the error vs. time was plotted. In these estimates, C_s was found to be an important a parameter which decided the accuracy of prediction. However, its contribution in T_c estimation was insignificant.

Sensitivity analysis for C_s was carried out. It was observed that low values of C_s showed minimal error in T_s estimation. Simulations were carried out for Case 1 for various values C_s as shown in Table 2.

Table 2. Sensitivity analysis of C_s for Case 1.

SL. NO	C_s (J/K)	Max Error ($T_{s\ estimation}$~$T_{s\ measured}$)
1	0.05	0.02
2	0.50	0.11
3	1.00	0.18
4	5.00	0.32

Figure 20a,b show the plots for inverse calculation for T_s estimation from known T_c for C_s = 0.05 and 12 J/K, respectively, for Case 1,and Figure 21a,b shows the error between the estimated and measured $T_{s,}$ respectively.

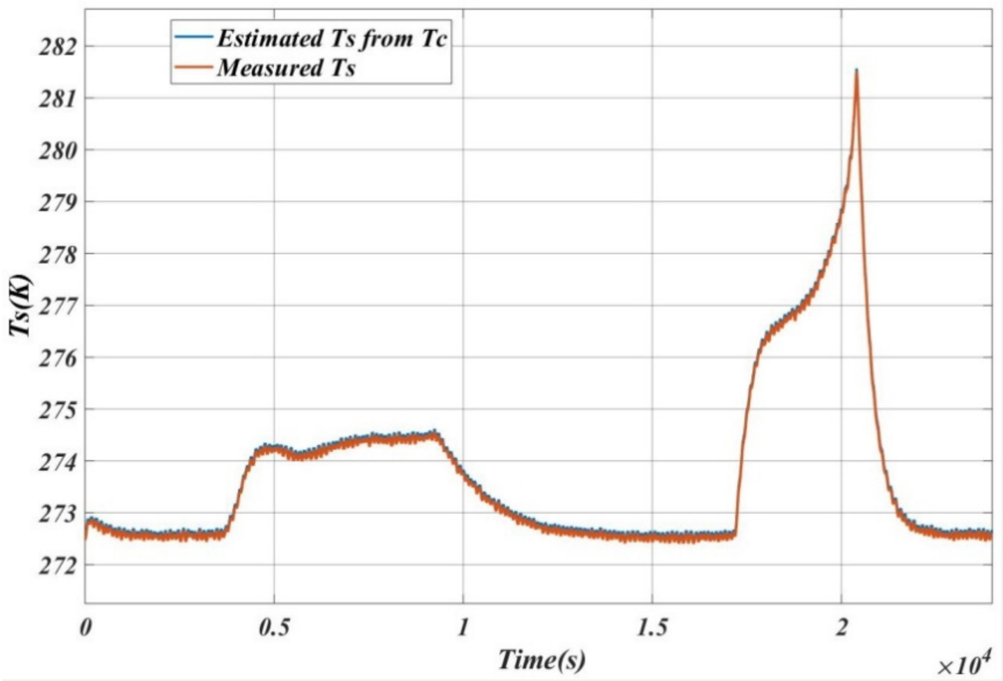

(**a**) C_s = 0.05 J/K

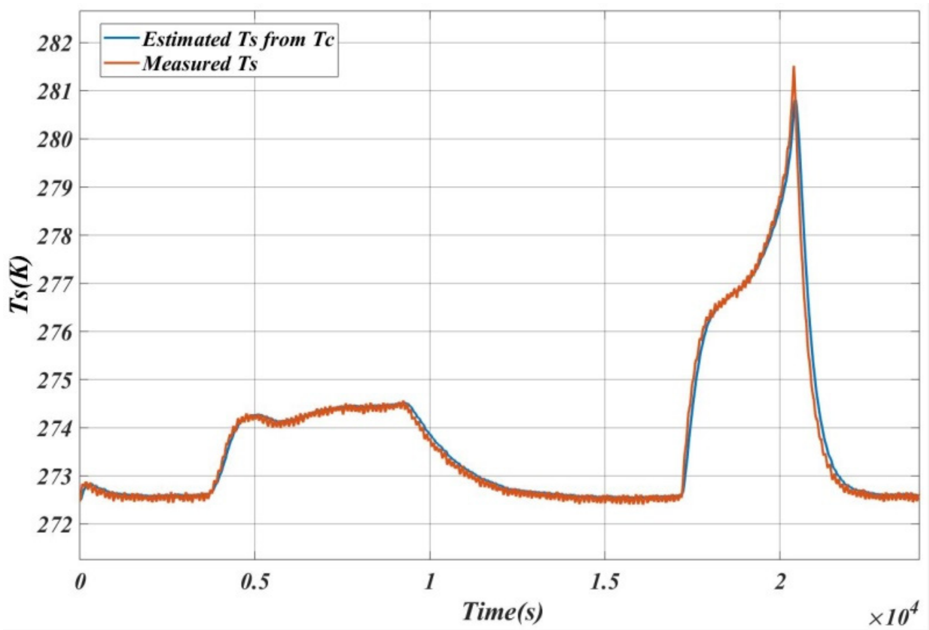

(**b**) C_s = 12 J/K

Figure 20. Variation of (estimated T_s − measured T_s) for various C_s.

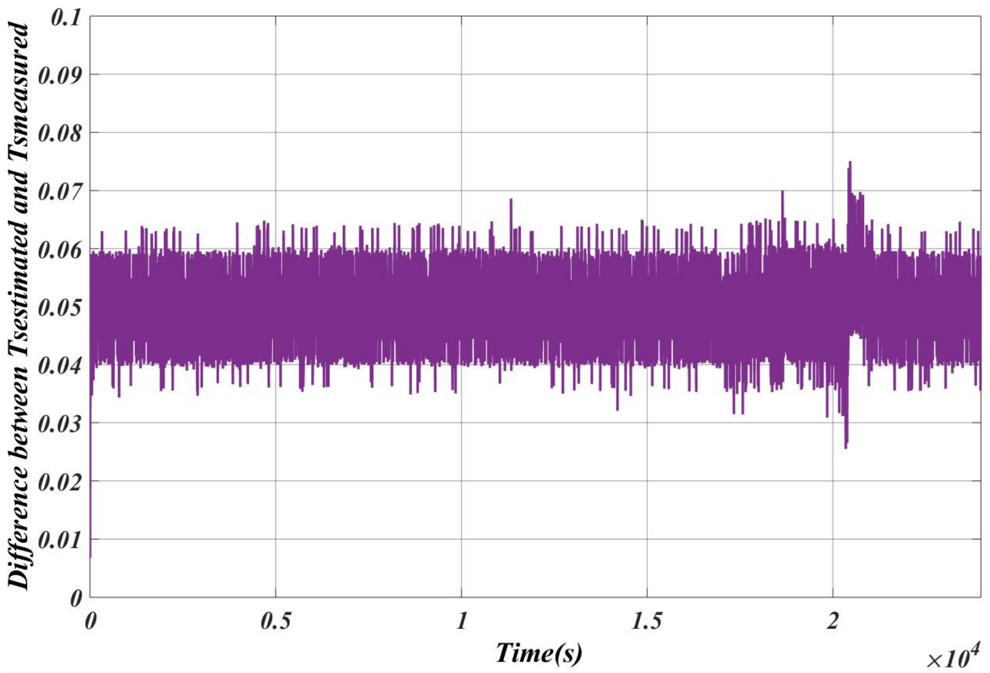

(**a**) C_s = 0.05 J/K

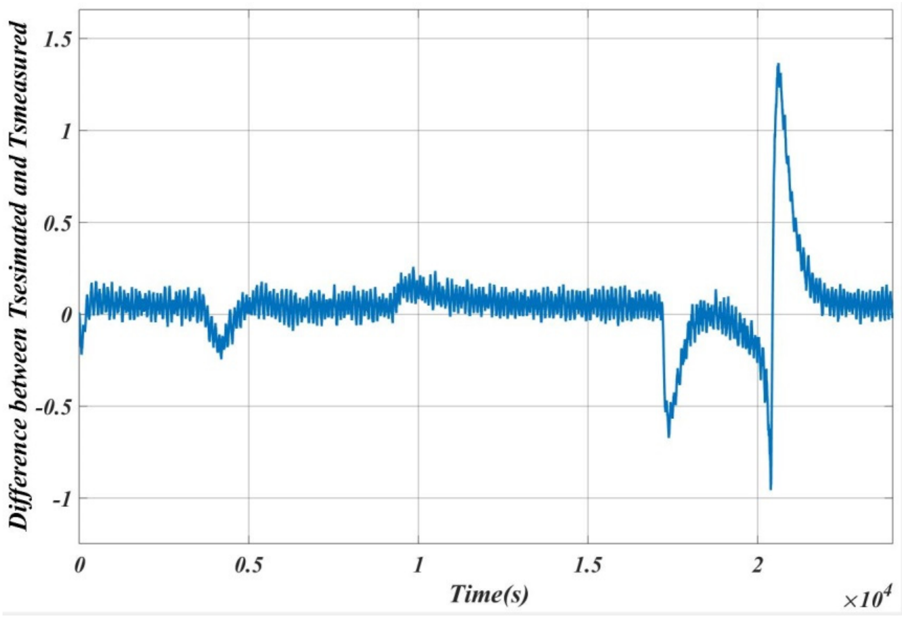

(**b**) C_s = 12 J/K

Figure 21. Error in estimation for various C_s.

Figure 22a,b shows the plots for inverse calculation for T_s estimation from known T_c for C_s = 0.05 and 12 J/K, respectively (Case 2), and Figure 23a,b shows their error in estimation, respectively.

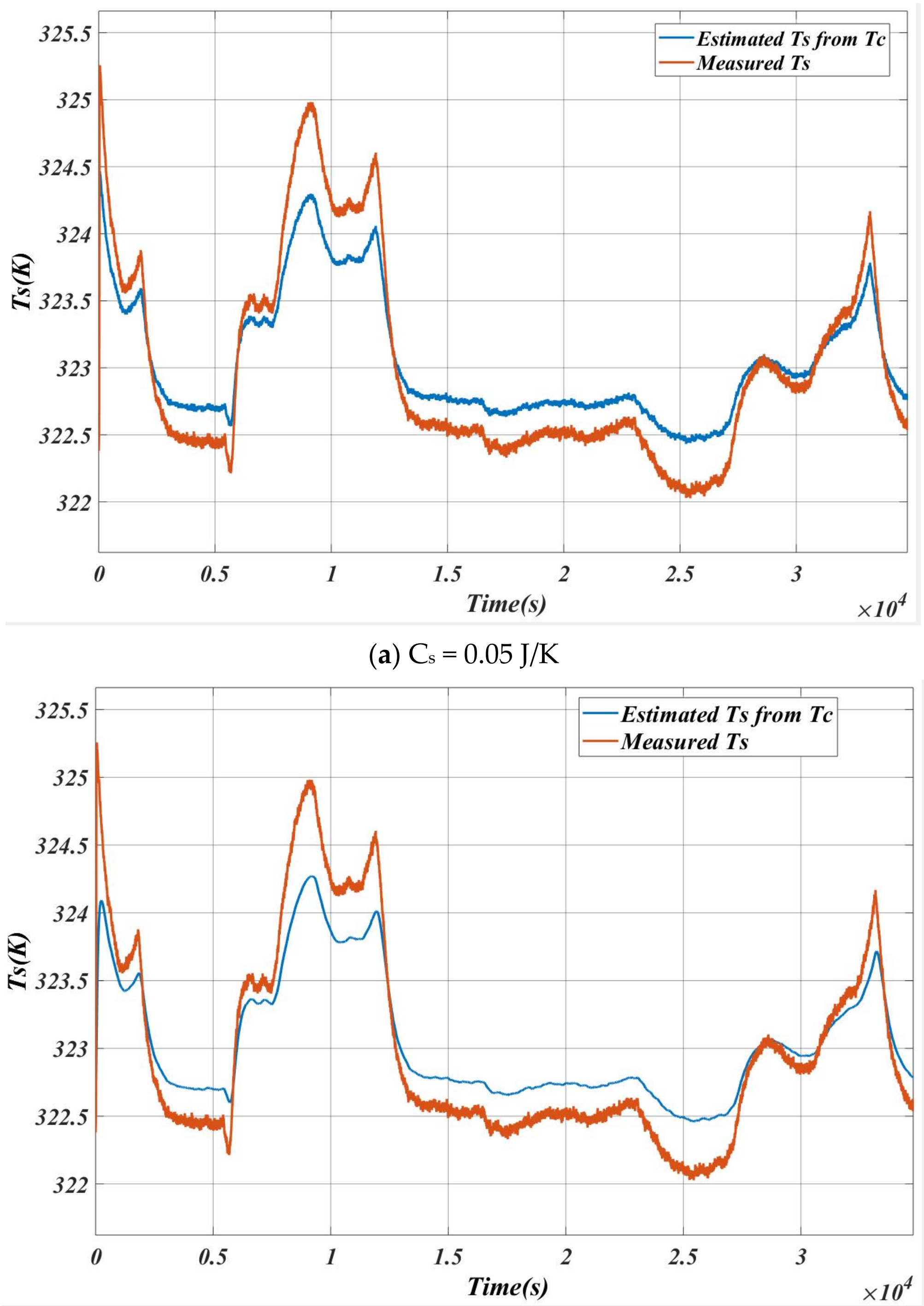

(**a**) C_s = 0.05 J/K

(**b**) C_s = 12 J/K

Figure 22. Variation of (estimated T_s − measured T_s) for various C_s.

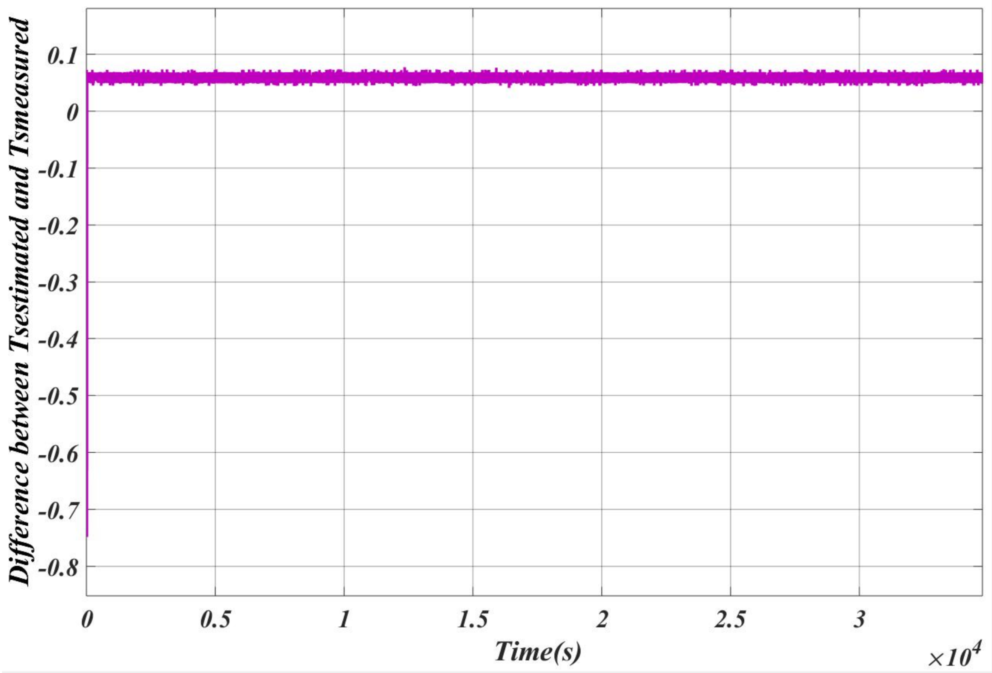

(**a**) C_s = 0.05 J/K

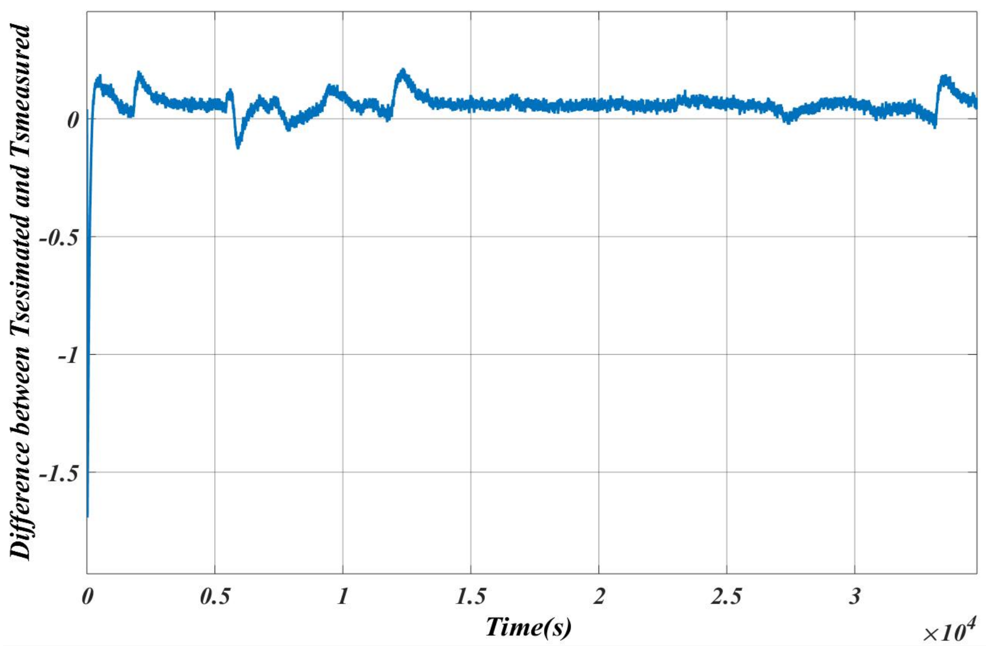

(**b**) C_s = 12 J/K

Figure 23. Error in estimation for various C_s.

Figure 24a,b shows the plots for inverse calculation for T_s estimation from known T_c for C_s = 0.05 and 12 J/K, respectively (Case 3) and Figure 25a,b shows their error in estimation, respectively.

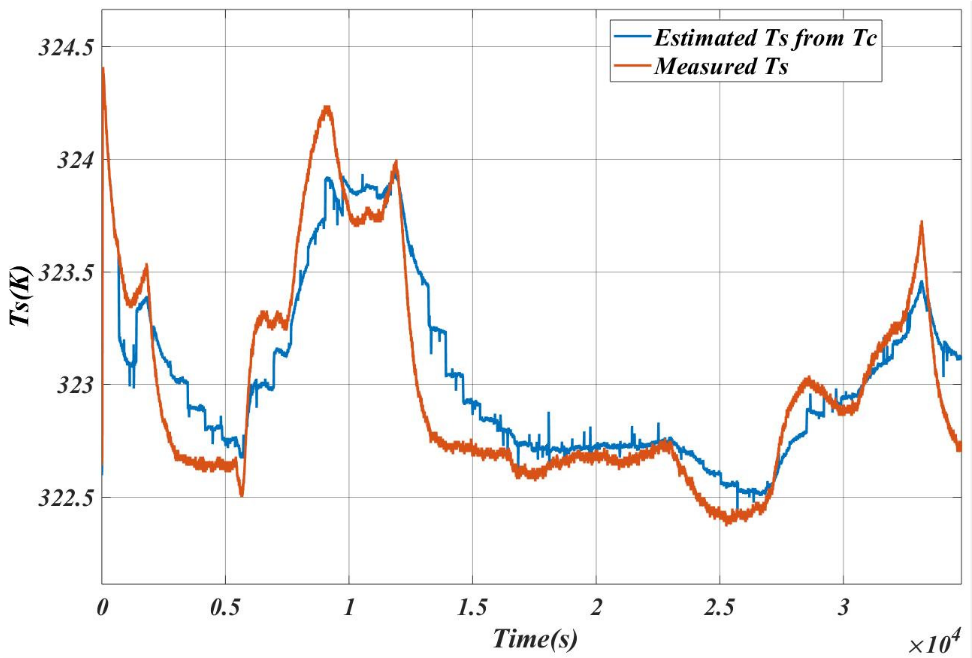

(**a**) C_s = 0.05 J/K

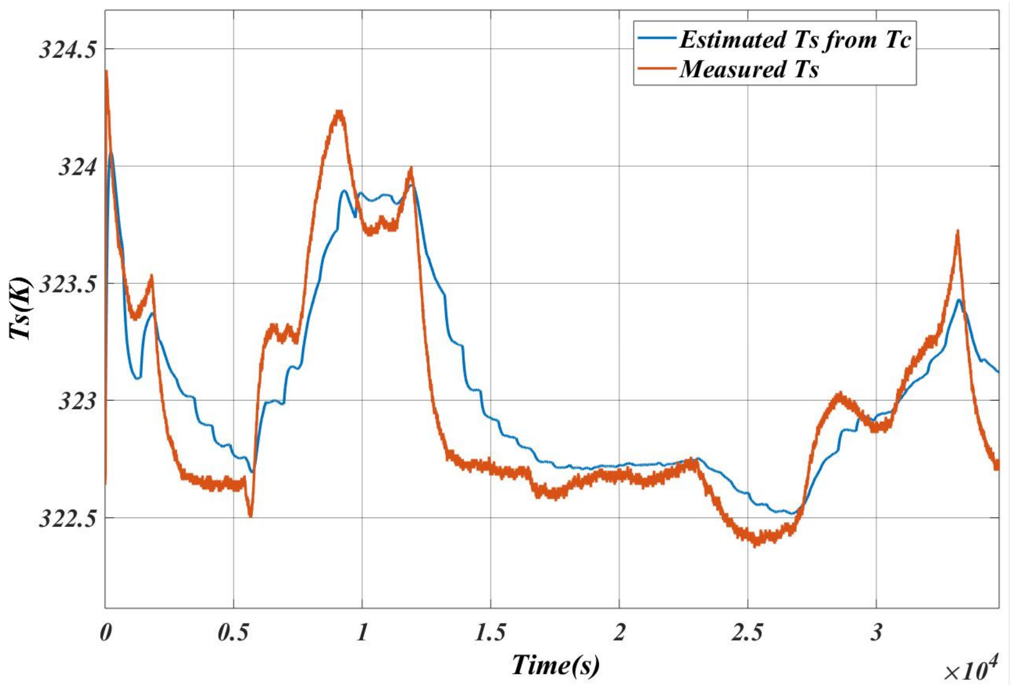

(**b**) C_s = 12 J/K

Figure 24. Variation of (estimated T_s − measured T_s) for various C_s.

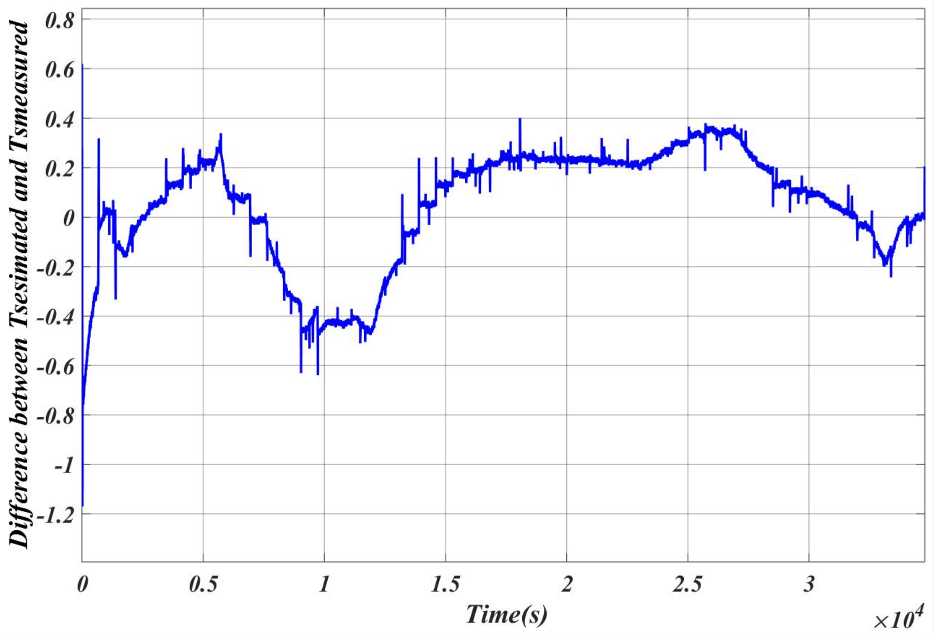

(**a**) C_s = 0.05 J/K

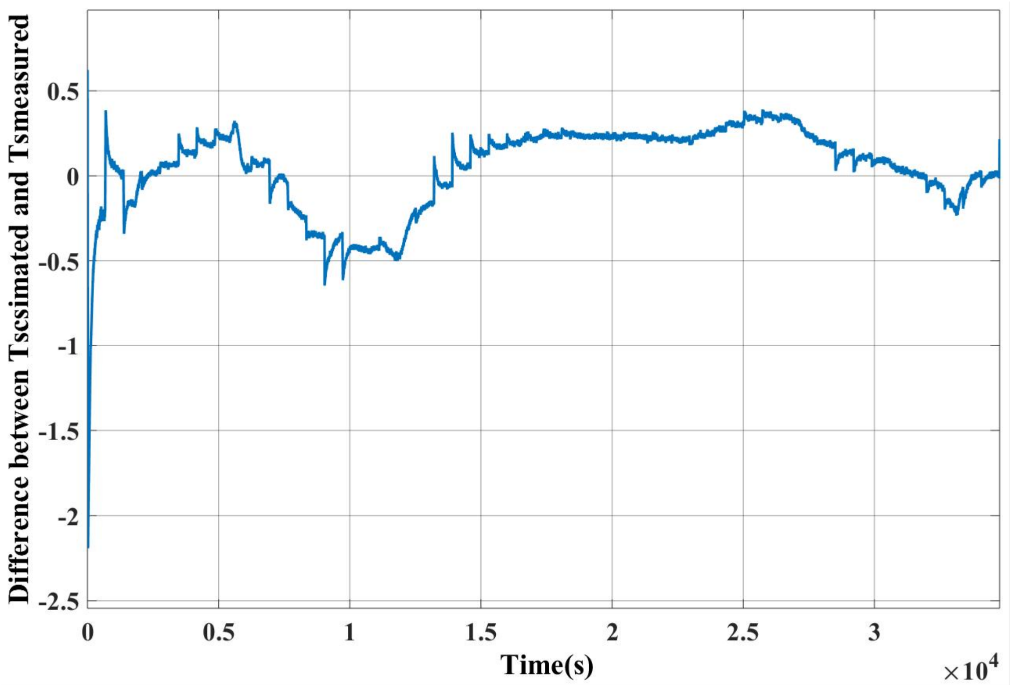

(**b**) C_s = 12 J/K

Figure 25. Error in estimation for various C_s.

Figure 26a,b shows the plots for inverse calculation for T_s estimation from known T_c for C_s = 0.05 and 12 J/K respectively (Case 4) and Figure 27a,b shows their error in estimation.

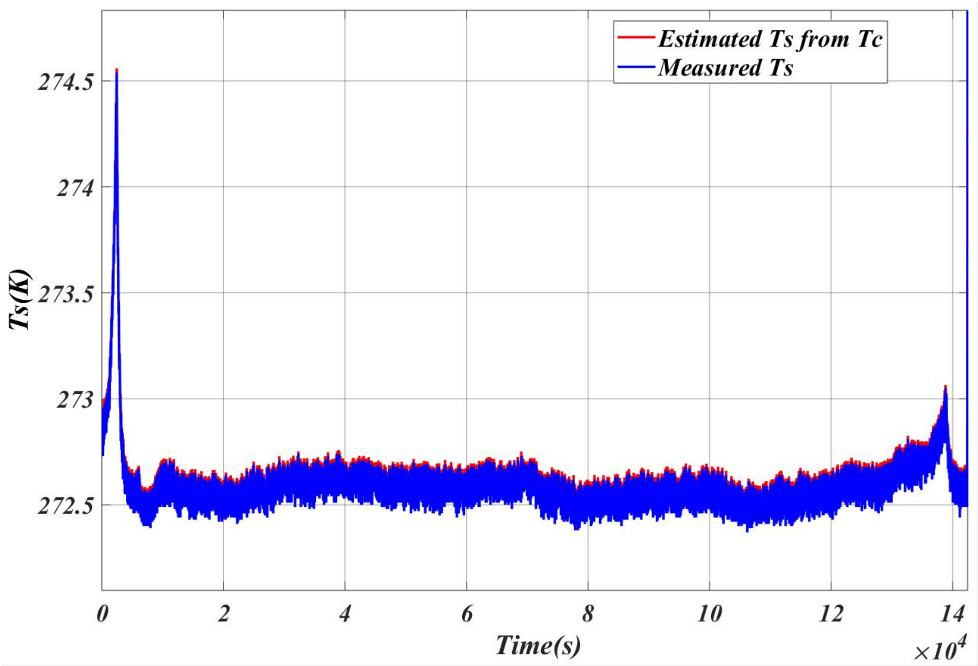

(**a**) C_s = 0.05 J/K

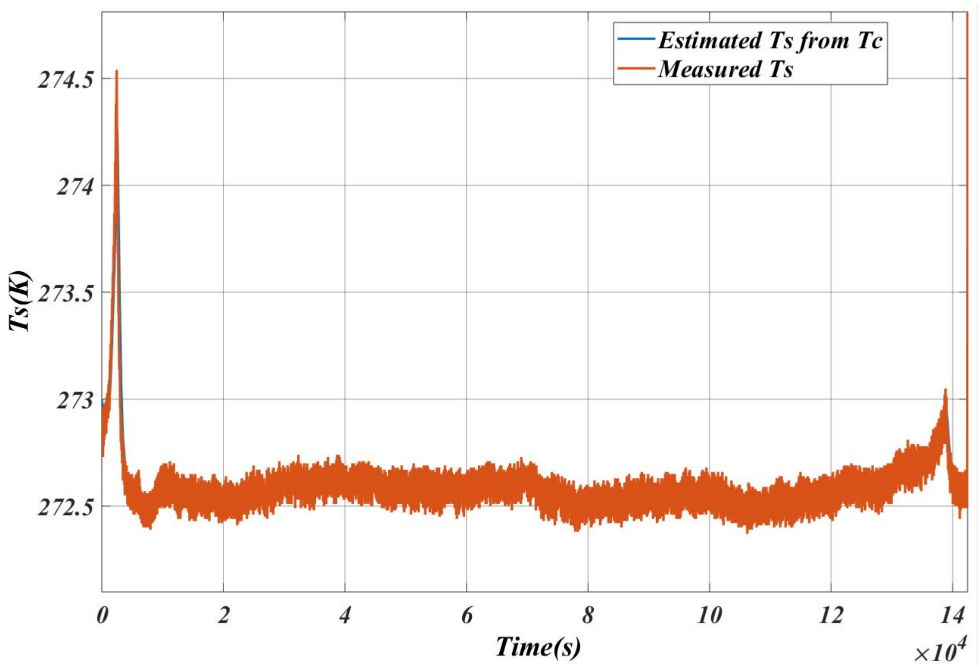

(**b**) C_s = 12 J/K

Figure 26. Variation of (estimated T_s − measured T_s) for various C_s.

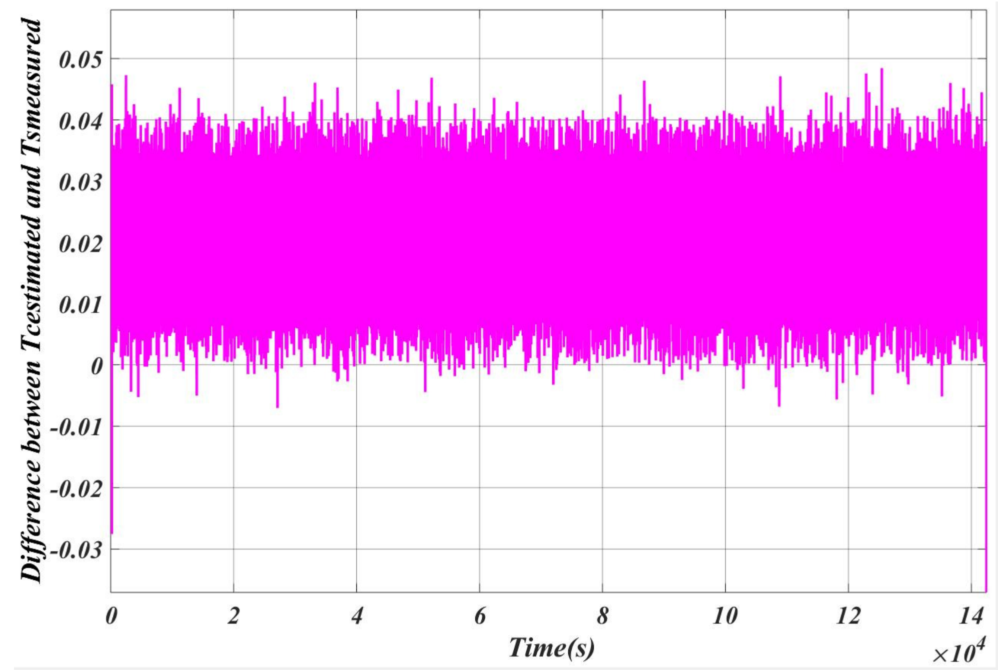

(**a**) C_s = 0.05 J/K

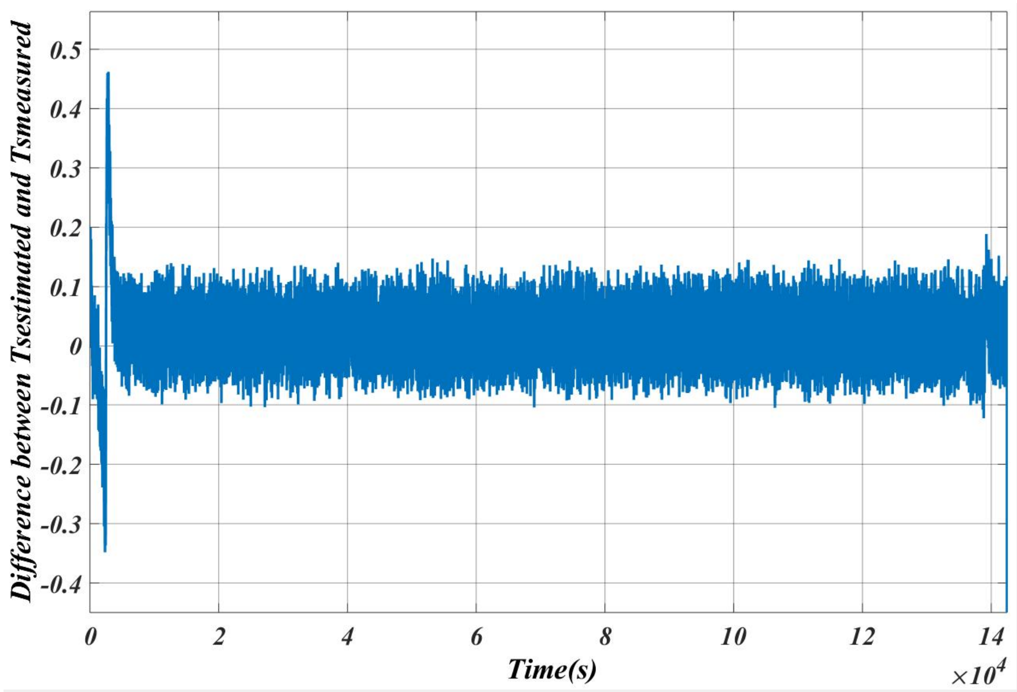

(**b**) C_s = 12 J/K

Figure 27. Error in estimation for various C_s.

It can be concluded from the above plots that smaller values of C_s provide better T_s estimates leading to minimum deviations. Table 3 shows a comparative percentage change in T_c for various types of batteries based on different current discharge profiles.

Table 3. Percentage change in T_c for various current discharge profiles.

SL.NO	Capacity (Ah)	Type of Chemistry	% Change in T_c
1	40	$LiFePO_4$	About 37
2	60	Lead acid	About 40
3	68	Lead acid	About 25
4	3	LiNiMnCo02HNMC	About 1

7. Conclusions

The governing equations for a thermal model were derived for a Li ion battery. Since, the sampling time was 1 s, the step size for solving the equation was chosen as 100 ms to capture transients. It was noted that $T_c > T_s$ whenever the magnitude of current discharge was large. The thermal capacitance C_s had no effect on the estimation of T_c. The thermal parameters chosen were R_c = 11.8 K/W, R_u = 10 K/W, C_c = 110 J/K. These values would depend on the order of the thermal model. The error percentage in estimating the thermal parameters for higher order thermal models with respect to the thermal model used would be <0.1%, which is acceptable. T_c estimation for higher order thermal models will be presented in the future papers. For every 273.25 K increase in temperature, battery capacity is affected by 5%. In order to avoid capacity fade, temperature has to be kept under control. Hence, T_c estimation is carried out. Inverse calculation was performed to obtain T_s from estimated T_c. For all BMS applications, the sensed temperature, T_s was used as an input for controller as homogeneity in T_s exits. Hence, inverse calculation was performed. Sensitivity was carried out and it was found that C_c and R_c majorly contributed to T_c. It was found that low values of C_s (0.05 J/K) provided minimal errors in estimation. As the value of C_s increased (C_s = 12 J/K), the error in estimations increased. Hence, optimization of C_s is an important contributor in inverse estimates.

Author Contributions: S.S.—Development of mathematical models for core temperature estimation and Kalman Filter using MATLAB/Simulink; V.M.—Carried out experimental work by measuring the battery current, ambient and surface temperatures using appropriate sensors; S.W.—Provided technical advice. All authors have read and agreed to the published version of the manuscript.

Funding: This research received no external funding.

Conflicts of Interest: The authors declare no conflict of interest.

Nomenclature

SL.No	Abbreviation	Meaning
1	T_{amb}	Ambient temperature
2	T_s	Surface temperature
3	T_c	Core temperature
4	R_c	Convective resistance between core and surface temperatures
5	R_u	Convective resistance between surface and ambient temperatures
6	C_c	Heat capacity of the core of the battery
7	C_s	Heat capacity of the surface of the battery
8	Q	Quantity of heat
9	I	Current

References

1. Plett, G.L. *Battery Management Systems, Volume I: Battery Modeling*; Artech House: Norwood, MA, USA, 2015.
2. Dai, H.; Zhu, L.; Zhu, J.; Wei, X.; Sun, Z. Adaptive Kalman filtering based internal temperature estimation with an equivalent electrical network thermal model for hard-cased batteries. *J. Power Sources* **2015**, *293*, 351–365. [CrossRef]
3. Baghdadi, I.; Briat, O.; Eddahech, A.; Vinassa, J.M.; Gyan, P. Electro-thermal model of lithium-ion batteries for electrified vehicles applications. In Proceedings of the 2015 IEEE 24th International Symposium on Industrial Electronics (ISIE), Rio de Janeiro, Brazil, 3–5 June 2015.

4. Machado, H.; Cicero, L.; Tanougast, C.; Ramenah, H.; Sieler, L.; Jean, P.; Milhas, P.; Dandache, A. VHDL-AMS electro-thermal modeling of a lithium-ion battery. In Proceedings of the 2013 25th International Conference on Microelectronics (ICM), Beirut, Lebanon, 15–18 December 2013.
5. Lin, X.; Perez, H.E.; Siegel, J.B.; Stefanopoulou, A.G.; Li, Y.; Anderson, R.D.; Ding, Y.; Castanier, M.P. Online parameterization of lumped thermal dynamics in cylindrical lithium ion batteries for core temperature estimation and health monitoring. *IEEE Trans. Control Syst. Technol.* **2012**, *21*, 1745–1755.
6. Surya, S.; Bhesaniya, A.; Gogate, A.; Ankur, R.; Patil, V. Development of thermal model for estimation of core temperature of batteries. *Int. J. Emerg. Electr. Power Syst.* **2020**. [CrossRef]
7. Patnaik, L.; Williamson, S. A Five-Parameter Analytical Curvefit Model for Open-Circuit Voltage Variation with State-of-Charge of a Rechargeable Battery. In Proceedings of the 2018 IEEE International Conference on Power Electronics, Drives and Energy Systems (PEDES), Madras, India, 18–21 December 2018.
8. Sumukh, S.; Janamejaya, C.; Abhay, S.J.; Shantanu, D.D.; Ashita, V. Accurate Battery Modeling Based on Pulse Charging using MATLAB/Simulink. In Proceedings of the Power Electronics Drives and Energy System (PEDES), Jaipur, India, 16–19 December 2020.
9. Mochnac, J.; Marchevsky, S.; Kocan, P. Bayesian filtering techniques: Kalman and extended Kalman filter basics. In Proceedings of the 19th International Conference Radioelektronika, Bratislava, Slovakia, 22–23 April 2009.
10. Brown, R.G.; Hwang, P.Y. *Introduction to Random Signals and Applied Kalman Filtering: With MATLAB Exercises*; John Wiley & Sons: New York, NY, USA, 2012; Volume 4.
11. Welch, G.; Gary, B. An Introduction to the Kalman Filter. Available online: http://www.ceri.memphis.edu/people/smalley/ESCI7355/welch%20and%20bishop%20-%20kalman.pdf (accessed on 25 December 2020).
12. Plett, G.L. *Battery Management Systems, Volume II: Equivalent-Circuit Methods*; Artech House: Norwood, MA, USA, 2015.
13. Tran, N.T.; Vilathgamuwa, M.; Farrell, T.; Li, Y.; Teague, J. A computationally-efficient electrochemical-thermal model for small-format cylindrical lithium ion batteries. In Proceedings of the 2018 IEEE 4th Southern Power Electronics Conference (SPEC), Singapore, 10–13 December 2018.
14. Sangiri, J.B.; Ghosh, S.; Chakraborty, C. Electro-thermal modeling of Lithium-ion cell for higher discharge rate applications. In Proceedings of the 21st Century Energy Needs-Materials, Systems and Applications (ICTFCEN), Kharagpur, India, 17–19 November 2016.
15. Hu, X.; Lin, S.; Stanton, S. A novel thermal model for HEV/EV battery modeling based on CFD calculation. In *2010 IEEE Energy Conversion Congress and Exposition*; IEEE: New York, NY, USA, 2010.
16. Surya, S.; Chennegowda, J.; Naraharisetti, K. Generalized Circuit Averaging Technique for Two Switch DC-DC Converters. In Proceedings of the 8th International Conference on Power Electronics Systems and Applications PESA, Hong Kong, China, 7–10 December 2020.
17. Richardson, R.R.; Howey, D.A. Sensorless Battery Internal Temperature Estimation Using a Kalman Filter With Impedance Measurement. *IEEE Trans. Sustain. Energy* **2015**, *6*, 1190–1199. [CrossRef]
18. Patnaik, L.; Praneeth, A.V.J.S.; Williamson, S.S. A Closed-Loop Constant-Temperature Constant-Voltage Charging Technique to Reduce Charge Time of Lithium-Ion Batteries. *IEEE Trans. Ind. Electron.* **2019**, *66*, 1059–1067. [CrossRef]
19. Marcis, V.A.; Praneeth, A.V.J.S.; Patnaik, L.; Williamson, S.S. Analysis of CT-CV Charging Technique for Lithium-ion and NCM 18650 Cells. In *2020 IEEE International Conference on Power Electronics, Smart Grid and Renewable Energy (PESGRE2020)*; IEEE: New York, NY, USA, 2020.